A butterfly-based direct solver using hierarchical LU factorization for Poggio-Miller-Chang-Harrington-Wu-Tsai equations

Article *in* Microwave and Optical Technology Letters · June 2018

DOI: 10.1002/mop.31166

CITATIONS
2

READS
66

4 authors, including:

Han Guo
University of Michigan
19 PUBLICATIONS **137** CITATIONS
SEE PROFILE

Yang Liu
Lawrence Berkeley National Laboratory
27 PUBLICATIONS **95** CITATIONS
SEE PROFILE

Jun Hu
University of Electronic Science and Technology of China
338 PUBLICATIONS **1,214** CITATIONS
SEE PROFILE

A butterfly-based direct solver using hierarchical LU factorization for PMCHWT equations

Han Guo[1] | Yang Liu[1] | Jun Hu[2] | Eric Michielssen[1]

[1] Department of Electrical Engineering and Computer Science, University of Michigan, Ann Arbor, MI 48109, USA

[2] Department of Microwave Engineering, University of Electronic Science and Technology of China, Chengdu, Sichuan 611731, China

Correspondence

Yang Liu, Department of Electrical Engineering and Computer Science, University of Michigan, Ann Arbor, MI 48109, USA.

Email: liuyangz@umich.edu

Abstract

A butterfly-based hierarchical LU factorization scheme for solving the PMCHWT equations for analyzing scattering from homogenous dielectric objects is presented. The proposed solver judiciously re-orders the discretized integral operator and butterfly-compresses blocks in the operator and its LU factors. The observed memory and CPU complexities scale as $O(N\log^2 N)$ and $O(N^{1.5}\log N)$, respectively. The proposed solver is applied to the analyses of scattering several large-scale dielectric objects.

KEYWORDS

fast direct solver, butterfly scheme, integral equation, homogenous dielectrics, scattering analysis, Poggio-Miller-Chang-Harrington-Wu-Tsai equation (PMCHWT)

1 | INTRODUCTION

The analysis of electromagnetic scattering from large-scale (piecewise) homogenous dielectric-magnetic objects oftentimes is performed using fast multipole-accelerated Poggio-Miller-Chang-Harrington-Wu-Tsai (PMCHWT) integral equation (IE) solvers[1,2]. Unfortunately, these iterative methods suffer from poor convergence when the object under study supports high-Q resonances or is discretized via dense meshes. They also become inefficient when applied to problems involving multiple excitations or requiring partial updates of discretized IE operators, further termed interaction matrices.

Fast direct solvers oftentimes outperform iterative ones under these conditions. With few exceptions, present direct solvers approximate off-diagonal blocks of interaction matrices and their "inverses" (e.g., LU factors and inverse decompositions leveraging H-matrix, hierarchically semi-separable matrix, and skeletonization techniques) using low-rank (LR) products[3,4,5,6,7,8,9]. These solvers exhibit quasi-linear CPU and memory requirements when applied to electrically small[3,10] and structured[11,12,13,14] objects. However, when used for analyzing scattering from electrically large and arbitrarily-shaped objects, their CPU and memory requirements deteriorate to $O(N^{\alpha}\log^{\beta} N)$ ($\alpha = 2.0 \sim 3.0$, $\beta \geq 1$) and $O(N^{\alpha}\log N)$ ($\alpha = 1.3 \sim 2.0$), as off-diagonal blocks of interaction matrices and their inverses are no longer LR compressible.

Recently, a new class of direct solvers leveraging butterfly compression schemes[15,16,17,18] was developed[19,20,21]. Butterfly schemes represent judiciously selected submatrices in off-diagonal blocks of interaction matrices (that are themselves LR incompressible) and their inverses in terms of LR products. The CPU and memory requirements of butterfly-based direct solvers for analyzing scattering from perfect electrically conducting (PEC) objects were estimated and experimentally validated to be $O(N^{1.5}\log N)$ and $O(N\log^2 N)$, irrespective of the object's shape and size[21].

This letter extends the above-referenced solver for PEC scatterers to homogeneous dielectric-magnetic objects. Specifically, it introduces a fast butterfly-enhanced hierarchical LU scheme for solving the PMCHWT equations. Butterfly compression is applied to blocks of a judiciously re-ordered PMCHWT interaction matrices, effectively combining four blocks in the original matrix into one that models a single (admissible) source-observer pair. The solver is applied to the analysis of scattering from a sphere, a NASA almond, and a helicopter model involving one million unknowns. Its CPU and memory requirements are observed to scale as $O(N^{1.5}\log N)$ and $O(N\log^2 N)$, respectively.

2 | FORMULATION

2.1 | PMCHWT Equations

Let Γ denote an arbitrarily-shaped closed surface with outward pointing normal $\hat{\boldsymbol{n}}$. The exterior and interior of Γ henceforth are termed regions 1 and 2. Region i = 1,2 has constant permittivity and permeability ε_i and μ_i, respectively. Time-harmonic electromagnetic fields $\{\boldsymbol{E}^{\text{inc}}(\boldsymbol{r}), \boldsymbol{H}^{\text{inc}}(\boldsymbol{r})\}$ with angular frequency ω produced by sources in region 1 impinge on Γ. Total electromagnetic fields $\{\boldsymbol{E}(\boldsymbol{r}), \boldsymbol{H}(\boldsymbol{r})\}$ are composed of incident and scattered fields, and relate to equivalent electric and magnetic currents $\boldsymbol{J}(\boldsymbol{r}) = \hat{\boldsymbol{n}} \times \boldsymbol{H}(\boldsymbol{r})$ and $\boldsymbol{M}(\boldsymbol{r}) = \boldsymbol{E}(\boldsymbol{r}) \times \hat{\boldsymbol{n}}$ on Γ that satisfy the PMCHWT equations

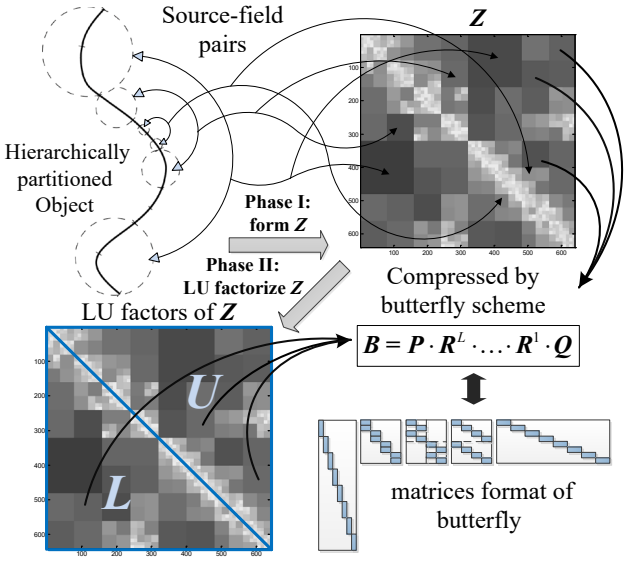

FIGURE 1 Matrix format of butterfly-based direct solver.

$$\mathcal{T}_1[\eta_1 \boldsymbol{J}](\boldsymbol{r}) + \frac{\eta_2}{\eta_1}\mathcal{T}_2[\eta_1 \boldsymbol{J}](\boldsymbol{r}) - \mathcal{K}_1[\boldsymbol{M}](\boldsymbol{r}) - \mathcal{K}_2[\boldsymbol{M}](\boldsymbol{r}) = -\hat{\boldsymbol{n}} \times \boldsymbol{E}^{\text{inc}}(\boldsymbol{r}) \tag{1}$$

$$\mathcal{K}_1[\eta_1 \boldsymbol{J}](\boldsymbol{r}) + \mathcal{K}_2[\eta_1 \boldsymbol{J}](\boldsymbol{r}) + \mathcal{T}_1[\boldsymbol{M}](\boldsymbol{r}) + \frac{\eta_1}{\eta_2}\mathcal{T}_2[\boldsymbol{M}](\boldsymbol{r}) = -\eta_1 \hat{\boldsymbol{n}} \times \boldsymbol{H}^{\text{inc}}(\boldsymbol{r}). \tag{2}$$

Here $\eta_i = \sqrt{\mu_i / \varepsilon_i}$ is the wave impedance in region i, and the operators $\mathcal{T}_i$ and $\mathcal{K}_i$ are

$$\mathcal{T}_i[\boldsymbol{F}](\boldsymbol{r}) = ik_i\eta_i \hat{\boldsymbol{n}} \times \int_\Gamma d\boldsymbol{r}' \boldsymbol{F}(\boldsymbol{r}') \cdot \left(\boldsymbol{I} - \frac{\nabla\nabla'}{k_i^2} \right) g_i(\boldsymbol{r}, \boldsymbol{r}') \tag{3}$$

$$\mathcal{K}_i[\boldsymbol{F}](\boldsymbol{r}) = -\hat{\boldsymbol{n}} \times P.V. \int_\Gamma d\boldsymbol{r}' \boldsymbol{F}(\boldsymbol{r}') \times \nabla' g_i(\boldsymbol{r}, \boldsymbol{r}') \tag{4}$$

where $\boldsymbol{I}$ is the identity dyad, $P.V.$ denotes Cauchy principal value, and $k_i = \omega\sqrt{\varepsilon_i \mu_i}$ and $g_i(\boldsymbol{r}, \boldsymbol{r}') = \exp(ik_i R)/(4\pi R)$ with $R = |\boldsymbol{r} - \boldsymbol{r}'|$ are the wavenumber and Green's function for region i, respectively.

To numerically solve (1) and (2), currents $\eta_1 \boldsymbol{J}(\boldsymbol{r})$ and $\boldsymbol{M}(\boldsymbol{r})$ are discretized using N' Rao-Wilton-Glisson (RWG) basis functions $\boldsymbol{f}_n(\boldsymbol{r})$ as[22]

$$\eta_1 \boldsymbol{J}(\boldsymbol{r}) = \sum_{n=1}^{N'} I_n^J \boldsymbol{f}_n(\boldsymbol{r}) \tag{5}$$

$$\boldsymbol{M}(\boldsymbol{r}) = \sum_{n=1}^{N'} I_n^M \boldsymbol{f}_n(\boldsymbol{r}). \tag{6}$$

Here I_n^J and I_n^M are electric and magnetic current expansion coefficients associated with $\boldsymbol{f}_n(\boldsymbol{r})$. Inserting (5)-(6) into (1)-(2) and testing the resulting equation with $\hat{\boldsymbol{n}} \times \boldsymbol{f}_n(\boldsymbol{r})$ yields the following $N \times N$ with $N = 2N'$ linear system of equations:

$$\begin{bmatrix} \boldsymbol{T}_1 + \frac{\eta_2}{\eta_1}\boldsymbol{T}_2 & -\boldsymbol{K}_1 - \boldsymbol{K}_2 \\ \boldsymbol{K}_1 + \boldsymbol{K}_2 & \boldsymbol{T}_1 + \frac{\eta_1}{\eta_2}\boldsymbol{T}_2 \end{bmatrix} \begin{bmatrix} \boldsymbol{I}^J \\ \boldsymbol{I}^M \end{bmatrix} = \begin{bmatrix} \boldsymbol{V}^E \\ \boldsymbol{V}^H \end{bmatrix}. \tag{7}$$

Here the n^{th} entries of $\boldsymbol{I}^J$ and $\boldsymbol{I}^M$ are I_n^J and I_n^M, respectively. The m^{th} entries of $\boldsymbol{V}^E$ and $\boldsymbol{V}^H$, $m = 1, ..., N'$, are

$$V_m^E = -\left\langle \hat{\boldsymbol{n}} \times \boldsymbol{f}_m(\boldsymbol{r}), \hat{\boldsymbol{n}} \times \boldsymbol{E}^{\text{inc}}(\boldsymbol{r}) \right\rangle \tag{8}$$

$$V_m^H = -\left\langle \hat{\boldsymbol{n}} \times \boldsymbol{f}_m(\boldsymbol{r}), \eta_1 \hat{\boldsymbol{n}} \times \boldsymbol{H}^{\text{inc}}(\boldsymbol{r}) \right\rangle \tag{9}$$

where $\langle \cdot, \cdot \rangle$ denotes the standard inner product. The $(m,n)^{\text{th}}$ elements of the interaction matrix follow from

$$T_{i,mn} = \left\langle \hat{\boldsymbol{n}} \times \boldsymbol{f}_m(\boldsymbol{r}), \mathcal{T}_i[\boldsymbol{f}_n](\boldsymbol{r}) \right\rangle \tag{10}$$

$$K_{i,mn} = \left\langle \hat{\boldsymbol{n}} \times \boldsymbol{f}_m(\boldsymbol{r}), \mathcal{K}_i[\boldsymbol{f}_n](\boldsymbol{r}) \right\rangle \tag{11}$$

The CPU and memory costs for directly solving (7) via Gaussian elimination or LU factorization scale as $O(N^3)$ and $O(N^2)$, respectively. Below, a butterfly-based hierarchical LU factorization scheme that reduces these requirements to $O(N^{1.5}\log N)$ and $O(N\log^2 N)$ is outlined. The scheme consists of two steps: filling/compressing and hierarchical LU factorization of the interaction matrix.

2.2 | Matrix Filling/Compression

The solver constructs a compressed representation of the interaction matrix in (7) via (i) recursive matrix decomposition and (ii) butterfly compression of off-diagonal blocks.

Step (i) recursively bisects Γ L^{M} times until the finest-level subscatterers contain $O(1)$ basis functions. At level $1 \le l \le L^{\text{M}}$, there are 2^l level $-l$ subscatterers, each containing roughly $N'/2^l$ basis functions. Two level $-l$ subscatterers constitute a far-field pair if their geometric centers are separated by at least $1 < \chi < 4$ times the sum of their circumscribing radii and their parent subscatterers do not form a far-field pair; two level $-L^{\text{M}}$ subscatterers that do not form a far-field pair constitute a near-field pair.

There are two unknowns (I_n^J and I_n^M) and two tested fields (V_n^E and V_n^H) associated with each function $\boldsymbol{f}_n(\boldsymbol{r})$. It follows there are four blocks in (7) associated with each subscatterer pair. To efficiently compress all blocks associated with one far-field pair, rows and columns in the interaction matrix in (7) are permuted, resulting in the following system of equations:

$$\boldsymbol{Z}\boldsymbol{I} = \boldsymbol{V}. \tag{12}$$

Here $\boldsymbol{I} = (I_1^J, I_1^M, ..., I_{N'}^J, I_{N'}^M)^T$, $\boldsymbol{V} = (V_1^E, V_1^M, ..., V_{N'}^E, V_{N'}^M)^T$ and

$$\boldsymbol{Z} = \boldsymbol{S}^T \begin{bmatrix} \boldsymbol{T}_1 + \frac{\eta_2}{\eta_1}\boldsymbol{T}_2 & -\boldsymbol{K}_1 - \boldsymbol{K}_2 \\ \boldsymbol{K}_1 + \boldsymbol{K}_2 & \boldsymbol{T}_1 + \frac{\eta_1}{\eta_2}\boldsymbol{T}_2 \end{bmatrix} \boldsymbol{S}. \tag{13}$$

And $\boldsymbol{S}$ denotes the permutation matrix that mixes the components of $\boldsymbol{I}^J$ and $\boldsymbol{I}^M$ into $\boldsymbol{I}$. In what follows, $\boldsymbol{Z}$ is termed the reordered interaction matrix. The recursive decomposi-

tion of Γ and unknown/field reordering procedures induce a hierarchical partitioning of the interaction matrix $\boldsymbol{Z}$ that is illustrated in Figure 1 for $L^{\mathrm{M}} = 7$ and Γ modeled by a 2D curve.

Step (ii) classically computes blocks representing near-field interactions via (10)-(11) and butterfly-compresses blocks representing far-field interactions. Consider a $m \times n$ level-l far-field block $\boldsymbol{Z}_S^O$ in $\boldsymbol{Z}$ with $n \approx m \approx N/2^l$. Note that odd/even indices in set S point to electric/magnetic unknowns I_n^J / I_n^M; similarly odd/even indices in set O point to measured fields in V_n^E / V_n^M. The butterfly scheme first divides $\boldsymbol{Z}_S^O$ into judiciously-selected submatrices $\boldsymbol{Z}_{S_i^d}^{O_j^d}$: for each $0 \le d \le L = L^M - l$, $i = 1,...,2^{L-d}$, $j = 1,...,2^d$, S_i^d and O_j^d are subsets corresponding to level-$l-L+d$ and level-$(l-d)$ subscatterers, respectively. It can be shown that the (butterfly) rank r of each submatrix $\boldsymbol{Z}_{S_i^d}^{O_j^d}$ is approximately constant[23]. Upon computing LR approximations to all $2^L(L+1)$ submatrices, the butterfly representation $\boldsymbol{B}$ of $\boldsymbol{Z}_S^O$ consists of the product of $L+2$ sparse matrices

$$\boldsymbol{B} = \boldsymbol{P}\boldsymbol{R}_L \ldots \boldsymbol{R}_1 \boldsymbol{Q} \tag{14}$$

where $\boldsymbol{P}$ and $\boldsymbol{Q}$ are block diagonal projection matrices, and the interior matrices $\boldsymbol{R}_d$, $d = 1,...,L$ are also block diagonal after (predefined) row permutation:

$$\boldsymbol{P} = \mathrm{diag}(\boldsymbol{P}_1,...,\boldsymbol{P}_{2^L}) \tag{15}$$

$$\boldsymbol{Q} = \mathrm{diag}(\boldsymbol{Q}_1,...,\boldsymbol{Q}_{2^L}) \tag{16}$$

$$\boldsymbol{D}_d \boldsymbol{R}_d = \mathrm{diag}(\boldsymbol{R}_{d,1},...,\boldsymbol{R}_{d,2^{L-1}}). \tag{17}$$

Here, $\boldsymbol{D}_d$ is the permutation matrix that yields $\boldsymbol{R}_d$ block diagonal, and the diagonal blocks in (15), (16) and (17) have approximate dimensions $(m/2^L) \times r$, $r \times (n/2^L)$, and $r \times 2r$ respectively (Figure 1).

It can be shown that construction and storage of one submatrix $\boldsymbol{Z}_S^O$ requires only $O(n \log n)$ CPU and memory resources, and that the overall memory and CPU requirements associated with the matrix filling phase scale as $O(N \log^2 N)$.

2.3 | Hierarchical LU Factorization

The second phase of the proposed solver constructs a butterfly-compressed hierarchical LU factorization of the reordered interaction matrix. The crux of the factorization process relies on the experimental observation that all blocks in the LU factors dimension-wise matching far-field blocks in $\boldsymbol{Z}$ are butterfly compressible with similar butterfly ranks. The solver arrives at a compressed representation of the LU factors of $\boldsymbol{Z}$ using randomized butterfly reconstruction methods to represent compositions of existing butterflies (additions, multiplications, and solutions of triangular systems) in terms of new butterflies.

The factorization process starts by partitioning and LU factorizing the impedance matrix $\boldsymbol{Z}$ as

$$\boldsymbol{Z} = \begin{bmatrix} \boldsymbol{Z}_{11} & \boldsymbol{Z}_{12} \\ \boldsymbol{Z}_{21} & \boldsymbol{Z}_{22} \end{bmatrix} = \begin{bmatrix} \boldsymbol{L}_{11} & \\ \boldsymbol{L}_{21} & \boldsymbol{L}_{22} \end{bmatrix} \begin{bmatrix} \boldsymbol{U}_{11} & \boldsymbol{U}_{12} \\ & \boldsymbol{U}_{22} \end{bmatrix} \tag{18}$$

The process proceeds as follows: (i) LU factorize $\boldsymbol{Z}_{11} = \boldsymbol{L}_{11}\boldsymbol{U}_{11}$; (ii) compute $\boldsymbol{U}_{12} = \boldsymbol{L}_{11}^{-1}\boldsymbol{Z}_{12}$ via back substitution; (iii) compute $\boldsymbol{L}_{21} = \boldsymbol{Z}_{21}\boldsymbol{U}_{11}^{-1}$ via back substitution; (iv) update $\hat{\boldsymbol{Z}}_{22} = \boldsymbol{Z}_{22} - \boldsymbol{L}_{21}\boldsymbol{U}_{12}$; and (v) LU factorize $\hat{\boldsymbol{Z}}_{22} = \boldsymbol{L}_{22}\boldsymbol{U}_{22}$. The constituent blocks in these five procedures are further partitioned until $\boldsymbol{Z}_{11}$, $\boldsymbol{Z}_{12}$, $\boldsymbol{Z}_{21}$, $\boldsymbol{L}_{21}/\boldsymbol{U}_{12}$, $\hat{\boldsymbol{Z}}_{22}$ in steps (i)-(v) dimension-wise match those in $\boldsymbol{Z}$. Consequently, the hierarchical partitioning of the LU factors of $\boldsymbol{Z}$ matches exactly that of $\boldsymbol{Z}$ (Figure 1).

During the recursive factorization process (i)-(v), there are essentially three types of block operations that are not recursive in nature:

$$\boldsymbol{B} = \boldsymbol{B}_1 + \boldsymbol{B}_2 \tag{19}$$

$$\boldsymbol{B} = \boldsymbol{B}_1 \cdot \boldsymbol{A} \text{ or } \boldsymbol{B} = \boldsymbol{A} \cdot \boldsymbol{B}_1 \tag{20}$$

$$\boldsymbol{B} = \hat{\boldsymbol{L}}^{-1} \cdot \boldsymbol{B}_1 \text{ or } \boldsymbol{B} = \boldsymbol{B}_1 \cdot \hat{\boldsymbol{U}}^{-1}. \tag{21}$$

Here $\boldsymbol{B}_1$ and $\boldsymbol{B}_2$ are butterfly-compressed matrices, and $\boldsymbol{A}$, $\hat{\boldsymbol{L}}$ and $\hat{\boldsymbol{U}}$ are hierarchical partitioned full, lower triangular, and upper triangular matrices with butterfly-compressed blocks. It is assumed and experimentally observed that all $\boldsymbol{B}$'s in (19)-(21) that dimension-wise match far-field blocks in $\boldsymbol{Z}$ can be butterfly-compressed. To arrive at butterfly approximations for all $\boldsymbol{B}$'s, the solver uses a fast randomized scheme that relies on the information gathered by (rapidly) multiplying $\boldsymbol{B}$ (i.e. the right hand sides in (19)-(21)) and its transpose to sparse random vectors[21].

The memory requirement of the factorization step scales as $O(N \log^2 N)$ due to the observation that butterfly ranks in (19)-(21) are approximately constant; the computational cost of the factorization step scales as $O(N^{1.5} \log N)$ because each randomized butterfly operation (19)-(21) requires $O(n^{1.5} \log n)$ CPU time. A detailed complexity analysis can be found in[21].

Once factorized, the inverse of the impedance matrix can be rapidly applied to excitation vectors using partitioned forward/backward substitution[3].

3 | NUMERICAL RESULTS

This section presents numerical results that demonstrate the efficiency and accuracy of the proposed solver. Simulations are performed on a cluster of eight-core 2.60 GHz Intel Xeon E5-2670 processors with 4 GB memory per core. In all examples, region 1 is vacuum, i.e. $\varepsilon_1 = \varepsilon_0$ and $\mu_1 = \mu_0$, the

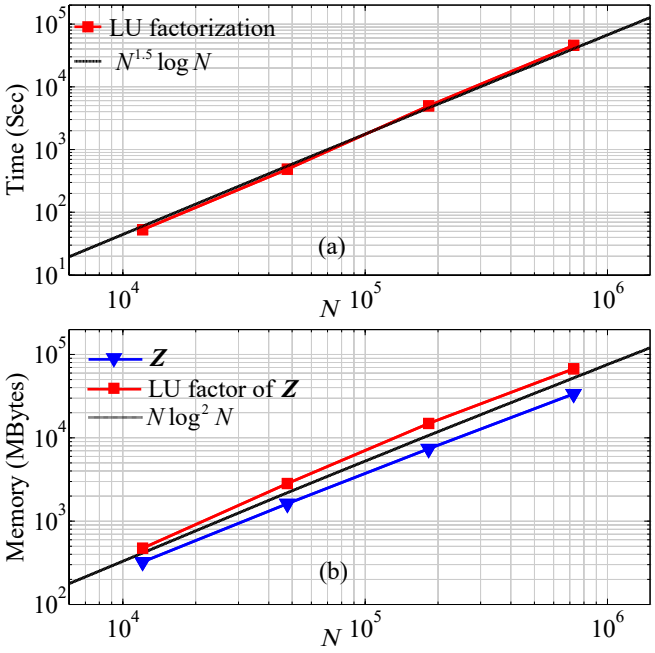

FIGURE 2 (a) Memory costs for storing $\boldsymbol{Z}$ and its LU factorization and (b) CPU times for the factorization phase using the proposed solver.

permittivity and permeability of the scatterers are $\varepsilon_2 = 3\varepsilon_0$ and $\mu_2 = \mu_0$, and χ is set to 2.

3.1 | Sphere

First, the memory and CPU requirements of the proposed solver are verified via its application to the analysis of scattering from a 1m-radius dielectric sphere. The frequency $f = \omega/(2\pi)$ and number of unknowns N are changed from 0.4 GHz and 12,072 to 3.2 GHz and 725,274, respectively. The solver utilizes 16 processors. The memory required to store $\boldsymbol{Z}$ and its LU factors, plotted in Figure 2(a), scale as $O(N\log^2 N)$. The CPU time required for factorizing $\boldsymbol{Z}$, shown in Figure 2(b), clearly adheres to the predicted $O(N^{1.5}\log N)$ scaling law.

Next, the accuracy of the proposed solver is demonstrated via computation of the sphere's bistatic radar cross section (RCS) for f = 3 GHz and $N = 961{,}008$. Matrix $\boldsymbol{Z}$ is hierarchically partitioned using 10 levels after setting the finest-level block dimension to approximately 938. The memory required for storing $\boldsymbol{Z}$ and its LU factors, and the CPU time required for filling and factorizing $\boldsymbol{Z}$ are listed in Table I. The solver requires peak memory of 853 GB and total CPU time of 82.6 h on 64 processors. The HH-polarized bistatic RCS in directions along $\theta = 90°$ and $\varphi = [0,180]°$ for a total of 10,000 directions are computed and compared with the Mie series solutions in Figure 3. Results agree very well.

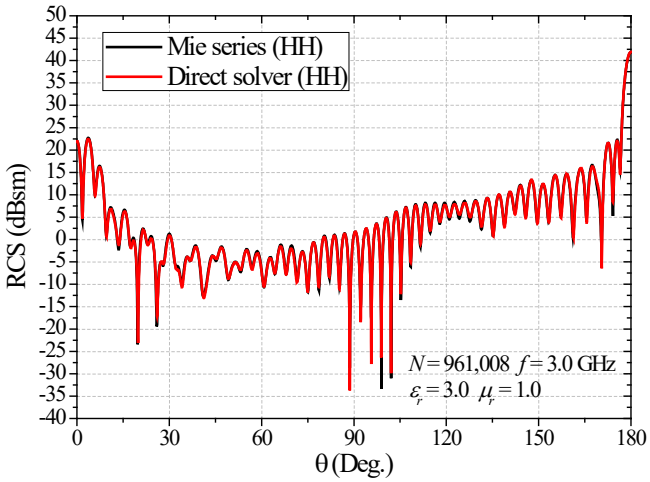

FIGURE 3 HH bistatic RCS of the sphere at 3 GHz computed at $\theta = 90°$ and $\varphi = [0,180]°$ using the proposed solver and the Mie series.

TABLE 1 The technical data for the setups and solutions of the largest scattering problems considered in this paper.

	Sphere	Almond	Helicopter
Max dimension	2 m (20 λ)	25 cm (33 λ)	22 m (36 λ)
Unknown N	961,008	722,712	559,992
Memory: $\boldsymbol{Z}$	493.1 GB	162.3 GB	111.5 GB
Memory: LU factor	853.5 GB	348.1 GB	383.1 GB
Matrix filling time	794 s	1.6 h	535 s
Factorization time	82.6 h	26.6 h	60 h
Solution time	136 s	37 s	65 s

3.2 | NASA Almond

Next, the proposed solver is applied to the analysis of scattering from a NASA almond enclosed by a fictitious box of dimensions $25.25\text{ cm} \times 9.76\text{ cm} \times 3.25\text{ cm}$. The almond is illuminated by a $f = 40.0$ GHz plane wave that is either x- or z-polarized and propagating along y. Matrix $\boldsymbol{Z}$ with $N = 722{,}712$ is partitioned using 9 levels by setting the finest-level block dimension to approximately 1411. The solver requires peak memory of 348 GB and total CPU time of 26.6 h using 64 processors (see Table I). The electric and magnetic currents induced on the almond are plotted in Figure 4.

3.3 | Helicopter

Finally, the proposed solver is applied to the analysis of scattering from a "plastic helicopter" model residing in a fictitious box of dimensions $18.60\text{ m} \times 21.96\text{ m} \times 7.15\text{ m}$. The helicopter is illuminated by a $f = 0.5$ GHz plane wave that is either x- or z-polarized and propagating along the y direction. The impedance matrix with $N = 559{,}992$ is hierarchically partitioned with 10 levels upon setting the size of the finest-level block dimension to approximately 546. The

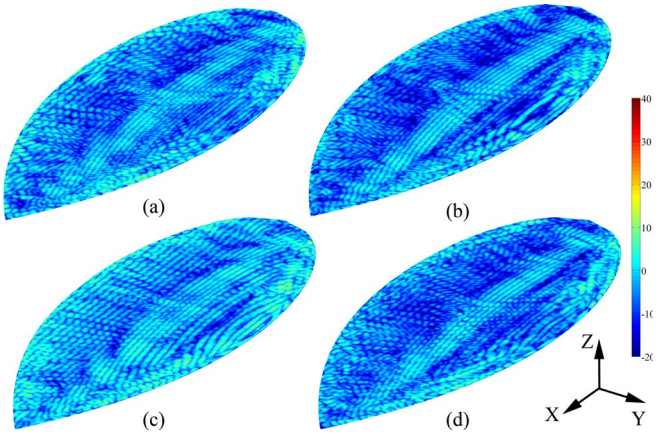

FIGURE 5 Current density (in dB) induced on the almond computed by the proposed direct solver: (a) $\eta_1 \boldsymbol{J}$ and (b) $\boldsymbol{M}$ induced by a *x*-polarized and -*y*-propagating incident electric field, and (c) $\eta \boldsymbol{J}$ and (d) $\boldsymbol{M}$ induced by a *z*-polarized and -*y*-propagating incident electric field.

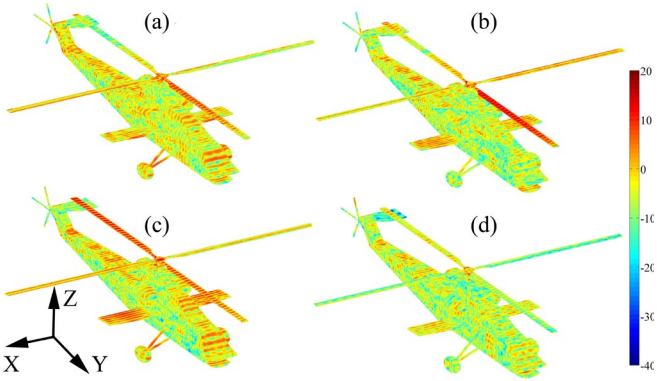

FIGURE 6 Current density (in dB) induced on the helicopter computed by the proposed direct solver: (a) $\eta_1 \boldsymbol{J}$ and (b) $\boldsymbol{M}$ induced by a *x*-polarized and -*y*-propagating incident electric field, and (c) $\eta \boldsymbol{J}$ and (d) $\boldsymbol{M}$ induced by a *z*-polarized and -*y*-propagating incident electric field.

memory requirements for storing $\boldsymbol{Z}$ and its LU factorization, and the CPU times for filling and factorizing $\boldsymbol{Z}$ as well as the backsubstitution phases are listed in Table I. The solver requires 383.1 GB memory and 60 h CPU time using 64 processors. The electric and magnetic currents on the helicopter are shown in Figure 5.

4 | CONCLUSIONS

A fast butterfly-based LU factorization scheme for solving the PMCHWT equations pertinent to the analysis of scattering from electrically large homogenous dielectric-magnetic objects was presented. The proposed solver re-orders and butterfly-compresses blocks in the interaction matrix and its LU factors. Importantly, the observed CPU and memory complexities of the resulting solver scale as $O(N^{1.5}\log N)$ and $O(N\log^2 N)$, respectively. Current efforts are aimed at reducing the leading constants implicit in the above estimates, to allow application of the solver to much bigger objects.

REFERENCES

[1] P. Yla-Oijala, M. Taskinen and S. Jarvenpaa, Analysis of surface integral equations in electromagnetic scattering and radiation problems, *Eng. Anal. Bound. Elem*, 2008;32:196-209.
[2] J. Song, C.-C. Lu and W.C. Chew, Multilevel fast multipole algorithm for electromagnetic scattering by large complex objects, *IEEE Trans. Antennas Propag.*, 1997;45:1488-1493.
[3] M. Bebendorf, Hierarchical LU decomposition-based preconditioners for BEM, *Computing*, 2005;74:225-247.
[4] J. Shaeffer, Direct solve of electrically large integral equations for problem sizes to 1 M unknowns, *IEEE Trans. Antennas Propag.*, 2008;56:2306-2313.
[5] W. Chai and D. Jiao, An-matrix-based integral-equation solver of reduced complexity and controlled accuracy for solving electrodynamic problems, *IEEE Trans. Antennas Propag.*, 2009;57:3147-3159.
[6] L. Greengard, D. Gueyffier, P.-G. Martinsson and V. Rokhlin, Fast direct solvers for integral equations in complex three-dimensional domains, *Acta Numerica*, 2009;18:243-275.
[7] A. Heldring, J.M. Rius, J.M. Tamayo, J. Parron and E. Ubeda, Multiscale compressed block decomposition for fast direct solution of method of moments linear system, *IEEE Trans. Antennas Propag.*, 2011;59:526-536.
[8] H. Guo, J. Hu, H. Shao and Z. Nie, Hierarchical matrices method and its application in electromagnetic integral equations, *Int. J. Antennas Propag.*, 2012;2012:
[9] J.-G. Wei, Z. Peng and J.-F. Lee, A fast direct matrix solver for surface integral equation methods for electromagnetic wave scattering from non-penetrable targets, *Radio Sci.*, 2012;47:
[10] E. Corona, P.-G. Martinsson and D. Zorin, An O(N) direct solver for integral equations on the plane, *Appl. Comput. Harmon. Anal.*, 2015;38:284-317.
[11] E. Michielssen, A. Boag and W. Chew, *Scattering from elongated objects: direct solution in O(N log 2 N) operations*, IEE P-Microw. Anten. P., IET, 1996, pp. 277-283.
[12] P.-G. Martinsson and V. Rokhlin, A fast direct solver for scattering problems involving elongated structures, *J. Comput. Phys.*, 2007;221:288-302.
[13] E. Winebrand and A. Boag, *A multilevel fast direct solver for EM scattering from quasi-planar objects*, Proc. Int. Conf. Electromagn. Adv. Appl., IEEE, 2009, pp. 640-643.
[14] Y. Brick, V. Lomakin and A. Boag, Fast direct solver for essentially convex scatterers using multilevel non-uniform grids, *IEEE Trans. Antennas Propag.*, 2014;62:4314-4324.
[15] E. Michielssen and A. Boag, A multilevel matrix decomposition algorithm for analyzing scattering from large structures, *IEEE Trans. Antennas Propag.*, 1996;44:1086-1093.
[16] E. Candes, L. Demanet and L. Ying, A fast butterfly algorithm for the computation of Fourier integral operators, *Multiscale Model. Sim.*, 2009;7:1727-1750.
[17] M. O'Neil, F. Woolfe and V. Rokhlin, An algorithm for the rapid evaluation of special function transforms, *Appl. Comput. Harmon. Anal.*, 2010;28:203-226.
[18] M. Tygert, Fast algorithms for spherical harmonic expansions, III, *J. Comput. Phys.*, 2010;229:6181-6192.
[19] Y. Liu, H. Guo and E. Michielssen, A HSS matrix-inspired butterfly-based direct solver for analyzing scattering from two-dimensional objects, *IEEE Antenn. Wireless Propag. Lett.*, 2016;
[20] H. Guo, J. Hu and E. Michielssen, On MLMDA/butterfly compressibility of inverse integral operators, *IEEE Antenn. Wireless Propag. Lett.*, 2013;12:31-34.
[21] H. Guo, Y. Liu, J. Hu and E. Michielssen, A butterfly-based direct integral equation solver using hierarchical LU factorization for analyzing scattering from electrically large conducting objects, *IEEE Trans. Antennas Propag.*, 2016;
[22] S.M. Rao, D.R. Wilton and A.W. Glisson, Electromagnetic scattering by surfaces of arbitrary shape, *IEEE Trans. Antennas Propag.*, 1982;30:409-418.
[23] O.M. Bucci and G. Franceschetti, On the degrees of freedom of scattered fields, *IEEE Trans. Antennas Propag.*, 1989;37:918-926.
[24] E. Michielssen and A. Boag, Multilevel evaluation of electromagnetic fields for the rapid solution of scattering problems, *Microw. Opt. Techn. Let.*, 1994;7:790-795.